J Toxicol Pathol 2017; 30: 291–306

Original Article

Ethanol extracts collected from the *Styela clava* tunic alleviate hepatic injury induced by carbon tetrachloride (CCl_4) through inhibition of hepatic apoptosis, inflammation, and fibrosis

Eun Kyoung Koh[1†], Ji Eun Kim[1†], Sung Hwa Song[1], Ji Eun Sung[1], Hyun Ah Lee[1], Kil Soo Kim[2], Jin Tae Hong[3], and Dae Youn Hwang[1*†]

[1] College of Natural Resources and Life Science/Life and Industry Convergence Research Institute, Pusan National University, 1268-50 Samnangjin-ro, Samnangjin-eup, Miryang-si, Gyeongsangnam-do 50463, Republic of Korea
[2] College of Veterinary Medicine, Kyungpook National University, 80 Daehak-ro, Buk-gu, Daegu 41566, Republic of Korea
[3] College of Pharmacy and Medical Research Center, Chungbuk National University, 1 Chungdae-ro, Seowon-gu, Cheongju-si, Chungcheongbuk-do 28644, Republic of Korea

Abstract: The *Styela clava* tunic (SCT) is known as a good raw material for preparing anti-inflammatory compounds, wound healing films, guided bone regeneration, and food additives. To investigate whether ethanol extracts of the SCT (EtSCT) could protect against hepatic injury induced by carbon tetrachloride (CCl_4) in ICR mice, alterations in serum biochemical indicators, histopathology, hepatic apoptosis, inflammation, and fibrosis were observed in ICR mice pretreated with EtSCT for 5 days before CCl_4 injection. EtSCT contained 15.6 mg/g of flavonoid and 37.5 mg/g phenolic contents with high 2,2-diphenyl-1-picrylhydrazyl (DPPH) radical scavenging activity (93.3%) and metal chelation activity (46.5%). The EtSCT+CCl_4-treated groups showed decreased levels of ALT, LDH, and AST, indicating toxicity and a necrotic area in the liver, while the level of ALP remained constant. The formation of active caspase-3 and enhancement of Bax/Bcl-2 expression was effectively inhibited in the EtSCT+CCl_4-treated groups. Furthermore, the levels of pro- and anti-inflammatory cytokines and the phosphorylation of p38 in the TNF-α downstream signaling pathway rapidly recovered in the EtSCT+CCl_4-treated groups. The EtSCT+CCl_4-treated groups showed a significant decrease in hepatic fibrosis markers including collagen accumulation, MMP-2 expression, TGF-β1 concentration, and phosphorylation of Smad2/3. Moreover, a significant decline in malondialdehyde (MDA) concentration and enhancement of superoxide dismutase (SOD) expression were observed in the EtSCT+CCl_4-treated groups. Taken together, these results indicate that EtSCT can protect against hepatic injury induced by CCl_4-derived reactive intermediates through the suppression of hepatic apoptosis, inflammation, and fibrosis. (DOI: 10.1293/tox.2017-0021; J Toxicol Pathol 2017; 30: 291–306)

Key words: hepatic injury, *Styela clava* tunic, inflammation, fibrosis, apoptosis, superoxide dismutase

Introduction

Hepatic fibrosis and inflammation are key factors promoting liver disease and subsequently leading to cirrhosis and hepatocellular carcinoma via regulation of cytokine secretion and recruitment of related cells[1, 2]. Hepatic fibrosis, the accumulation of extracellular matrix or scars, is a wound healing response to acute or chronic liver injury induced by various disease conditions including viral, autoimmune, drug-induced, cholestatic, and metabolic diseases. This condition ultimately leads to cirrhosis[3]. The end-stage consequence of fibrosis was found to be altered hepatic function and blood flow via nodule formation[3]. Moreover, most patients with compensated cirrhosis often progress to hepatocellular carcinoma[4]. Hepatic inflammation is a key regulator of the progression of hepatic fibrosis to cirrhosis and hepatocellular carcinoma through regulation of various signaling pathways[5, 6]. Therefore, the suppression of hepatic fibrosis and inflammation is important to prevent the occurrence of hepatocellular carcinoma and liver cirrhosis.

Many natural products have recently received attention as hepatoprotective sources with antioxidant activity because they can successfully overcome some limitations, including the large-scale procurement of sufficient source materials for bulk production, the potency and inherent toxicity of many natural products, and the development of suitable vehicles and dosing schedules for the administration of new drugs to clinical patients[7]. Among these products,

Received: 22 March 2017, Accepted: 29 June 2017
Published online in J-STAGE: 28 August 2017
*Corresponding author: DY Hwang, (e-mail: dyhwang@pusan.ac.kr)
†These authors contributed equally to this work.

we focused on the protective effects of the *Styela clava* tunic (SCT) as part of studies evaluating the possibility of use of novel bioactive materials and providing solutions for the problems associated with SCT waste[8, 9]. To date, the SCT has been extensively applied to purification of natural polymers and bioactive compounds for the treatment of inflammation, oxidative stress, and surgical wounds. A cellulose complex derived from the SCT showed good healing effects on surgical wounds and bone defects in animals. Cellulose films (CFs) prepared using N-methylmorpholine-N-oxide (NMMO)/H_2O (87/13 wt%) did not induce epidermal hyperplasia, inflammatory cell infiltration, redness, or edema after application to surgical wounds for 2 weeks[10, 11]. In addition, SD rats with surgical wounds treated with a hydrocolloid membrane containing SCT (HCM-SCT) showed significantly faster reepithelialization, decreased epidermis thickness, shorter wound diameter, and increased collagen[12]. Bioactive effects on bone and mesenchymal tissues were also observed in the periosteum of cervical bone defects of SD rats treated with a cellulose membrane (CM) obtained from *Ascidians* (squirt) skin[13].

Several bioactive compounds and extracts collected from the SCT by extraction with different solvents have also been found to have biological activity in cells and animals. TNF-α-induced NF-κB activation and the expression of two inflammatory factors (VCAM-1 and iNOS) were effectively suppressed by chondroitin sulfate extracted from the SCT in JB6 P^+ cells derived from BALB/c mice[14]. Moreover, carotenoids detected at high levels in the SCT showed strong hydroxyl radical scavenging activities, reducing power, and inhibitory effects against linoleic acid peroxidation[15]. High levels of tyrosinase inhibition and antioxidant activity were also induced by nine extracts collected from the SCT using different solvents, as because they have high total phenolic and flavonoid contents[9]. However, the protective effects and their mechanisms against hepatotoxicity induced by oxidative stress after toxic chemical treatment have not yet been investigated in animal models, although extracts obtained from the tunic of other species within the subphylum Urochordata have been shown to have significant hepatoprotective effects.

Therefore, in this study, we investigated the protective effects of ethanol extracts of the SCT (EtSCT) against mouse hepatic injury induced by CCl_4 treatment. The results presented herein provide the first evidence that EtSCT can protect against the enhancement of serum biochemical markers of liver toxicity, histopathology, apoptosis, inflammation, and fibrosis that occurs after CCl_4 treatment through suppression of reactive intermediates and upregulation of antioxidant enzymes.

Materials and Methods

Collection of SCTs and preparation of EtSCT

SCT powder was prepared as previously described[16], and voucher specimens of SCTs (WPC-14-002) were deposited in the functional materials bank of the Pusan National University (PNU)-Wellbeing Regional Innovation System (WRIS) Center. Briefly, dry samples of SCT (330 g) were boiled in 10% NaOH aqueous solution (9,900 ml) at 100°C for 2 h to remove sediments and debris after harvesting from a beach along of the South Sea in Gosung-gun, Republic of Korea. After washing, samples were further boiled in 5% CH_3COOH solution at 100°C for 2 h to neutralize the NaOH solution and then washed with distilled water three times. The SCTs were subsequently bleached by separate boiling and washing in 10% H_2O_2 solution. After a final wash with distilled water, samples were dried at 100–120°C for 2–3 h and then ground in a pin mill machine (Daehwa, Republic of Korea) using a proprietary commercial process in which they were passed through a combination of 30 mesh sieves over the course of 10 min one time and then through a combination of 120 mesh sieves over the course of 10 min twice.

EtSCT were prepared from SCT powder according to methods established in our laboratory[9]. Briefly, ethanol extracts were purified from 100 g of SCT powder over the course of 3 h at 80°C using circulating extraction equipment (IKA-Werke GmbH & Co. KG, Staufen im Breisgau, Germany) after adding 1,000 ml of 100% ethanol. After repeating this process three times, the extracts were concentrated into dry pellets in a rotary evaporator (EYELA, Tokyo, Japan) following filtration through filter paper (Whatman No. 1, 100–125, Whatman International Ltd., Maidstone, England). Finally, EtSCT were stored at −80°C until further use (Fig. 1A).

Measurement of total phenolic and flavonoid contents

To measure the total phenolic contents, we used the Folin-Ciocalteu method with slight modification[17]. Briefly, 1 ml of EtSCT solution was mixed with 5 ml of Folin-Ciocalteu reagent (Sigma-Aldrich Corporation, St. Louis, MO, USA) and then incubated at room temperature for 5 min. The mixture was subsequently added to 15 ml of 20% Na_2CO_3 and vortexed for 30 sec, after which the absorbance was repeatedly measured at 765 nm using a VersaMax plate reader (Molecular Devices, Sunnyvale, CA, USA). A standard calibration curve was made using different concentrations of gallic acid (Sigma-Aldrich Corporation), and the concentration of total phenolic contents in EtSCT was presented as mg gallic acid equivalent of extract.

Flavonoid contents were measured as previously described[18]. Briefly, several different concentrations of EtSCT (200 μl) were mixed with 60 μl of 5% $NaNO_2$ (Sigma-Aldrich Corporation) and 60 μl of 10% $AlCl_3$ (Sigma-Aldrich Corporation). Following incubation at 25°C for 5 min, the mixture was added to 400 μl of 1 M NaOH, and the absorbance was repeatedly measured at 510 nm using a VersaMax plate reader (Molecular Devices). A standard calibration curve was then made using different concentrations of catechin (Sigma-Aldrich Corporation). The final concentration of flavonoid contents in EtSCT was presented as mg catechin equivalent of extract.

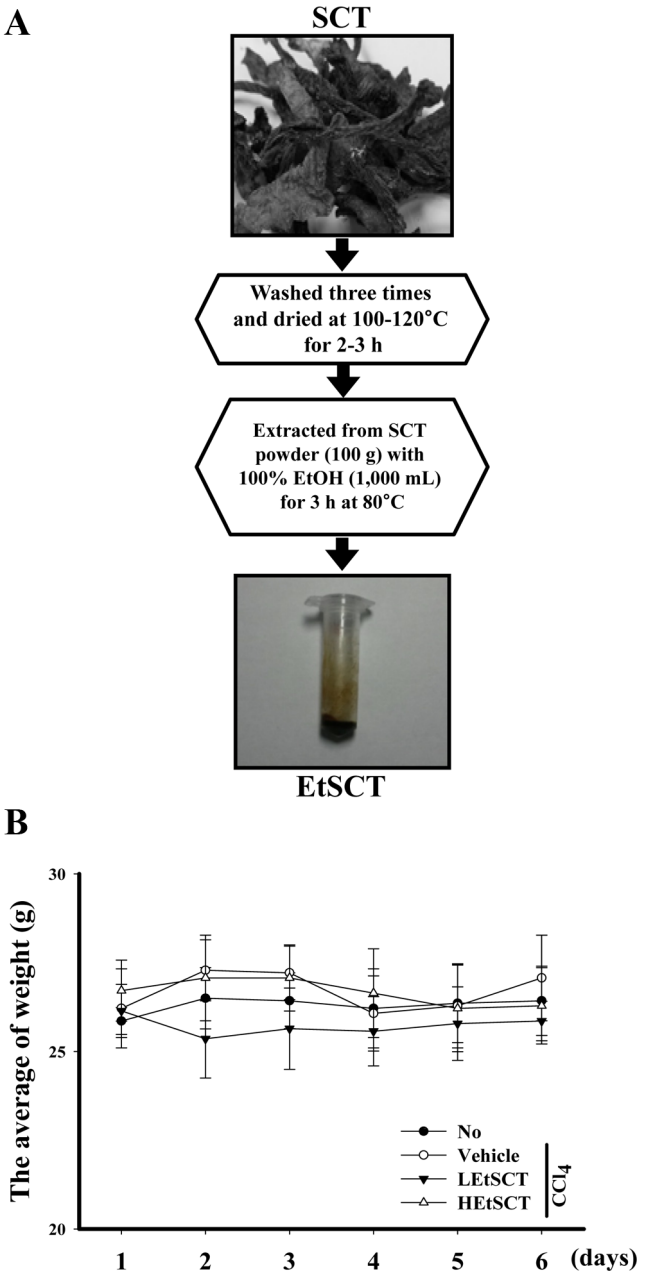

Fig. 1. Preparation of EtSCT and alteration of body weight of ICR mice treated with EtSCT. (A) EtSCT was prepared by serial processing consisting of bleaching, neutralizing, milling, and extraction as described in the Materials and Methods. (B) The body weights of subset groups were measured throughout the experimental period. The data shown represent the means ± SD of three replicates.

Analysis of antioxidant activity

The scavenging activity of DPPH radicals was measured as previously described[19]. Briefly, each sample (250 µl) of EtSCT was mixed with 500 µL of 0.2 mM DPPH (Sigma-Aldrich Corporation) in 95% ethanol solution or 100 µL of 95% ethanol solution and then incubated for 30 min at room temperature. Next, the absorbance of the reaction mixture was measured at 517 nm using a VersaMax plate reader (Molecular Devices). The DPPH radical scavenging activity of the EtSCT was expressed as the percent decrease in absorbance relative to the control.

The reducing power of EtSCT was determined as previously described[20]. Briefly, an appropriate volume (250 µl) of EtSCT solution was mixed with 250 µl of 0.2 M sodium phosphate buffer (pH 6.6) and 250 µl of 1% potassium ferricyanide and then incubated at 50°C for 20 min. Following centrifugation at 1,000 × g for 10 min, the supernatant was collected (250 µl) and mixed with 50 µl of distilled water and 50 µl of 0.1% ferric chloride and it was then incubated at room temperature for 10 min. Finally, the absorbance of the reaction mixture was measured at 700 nm using a VersaMax plate reader (Molecular Devices). The reducing power was reported as the percentage increase in rate of absorbance of the EtSCT-treated group relative to the absorbance level of a DMSO-treated group.

The scavenging activity of nitric oxide (NO) was measured as previously described[21]. Briefly, each sample of EtSCT (500 µl) was mixed with 500 µL of 10 mM sodium nitroprusside (Sigma-Aldrich Corporation) and then incubated at 25°C for 150 min. This mixture was subsequently added to 500 µl of 1% sulfanilamide solution and 500 µl of 0.1% N-(1-naphthyl) ethylenediamine dihydrochloride solution and incubated at room temperature for 10 min. The absorbance of the reaction mixture was subsequently measured at 546 nm using a VersaMax plate reader (Molecular Devices). The NO scavenging activity of the EtSCT was expressed as the percentage absorbance relative to a control treated with dimethyl sulfoxide (DMSO, Daejung Chemicals & Metals Co., Ltd, Siheung, Republic of Korea).

The metal chelation activity of EtSCT was measured as previously described[9, 22]. Briefly, each sample of EtSCT (1 ml) was mixed with 100 µL of 5 mM ferrous chloride (Sigma-Aldrich Corporation) and 200 µL of 5 mM ferrozine (Sigma-Aldrich Corporation). Following incubation at 25°C for 10 min, the absorbance of the reaction mixture was measured at 546 nm using a VersaMax plate reader (Molecular Devices). Finally, the metal chelation activity of the EtSCT was expressed as the percentage absorbance relative to a control treated with DMSO (Daejung Chemicals & Metals Co.).

SOD-like activity was measured as previously described[23]. Briefly, 200 µL of EtSCT sample was mixed with 3 mL of 50 mM Tris-HCl and 200 µL of 7.2 mM pyrogallol (Sigma-Aldrich Corporation) and then incubated at 25°C for 10 min. The absorbance of the reaction mixture was subsequently measured at 546 nm using a VersaMax plate reader (Molecular Devices). Furthermore, the SOD-like activity of the EtSCT was expressed as the percentage absorbance relative to a control treated with DMSO (Daejung Chemicals & Metals Co.).

Animal experiment

The animal protocols applied in our study were reviewed and approved by the Pusan National University Institutional Animal Care and Use Committee (PNU-

IACUC; Approval Number: PNU-2014-0594). All mice were handled in the Pusan National University Laboratory Animal Resources Center, which is accredited by the Korea Food and Drug Administration (FDA; Accredited Unit Number: 000231) and AAALAC International (Accredited Unit Number: 001525). Ten-week-old male ICR mice were purchased from Samtako BioKorea Co. (Osan, Republic of Korea) and provided with *ad libitum* access to water and a standard irradiated chow diet (Samtako BioKorea Co.) consisting of moisture (12.5%), crude protein (25.43%), crude fat (6.06%), crude fiber (3.9%), crude ash (5.31%), calcium (1.14%), and phosphorus (0.99%) throughout the feeding study. During the experiment, mice were maintained in a specific pathogen-free state under a strict light cycle (lights on at 08:00 h and off at 20:00 h) at 23 ± 2°C and 50 ± 10% relative humidity.

Total ICR mice (28 mice) were divided into the following four groups (n=7 per group): a non-treated group, Vehicle+CCl_4-treated group, low concentration of EtSCT (LEtSCT)+CCl_4 treated-group, and high concentration of EtSCT (HEtSCT)+CCl_4-treated group. The first group did not receive any solution throughout the study period, while the second group repeatedly received a constant volume of desterilized water. The other two groups were treated with 50 mg (LEtSCT+CCl_4-treated group) and 100 mg (HEtSCT+CCl_4-treated group) of EtSCT per kg of body weight/day during the same period because these doses did not induce any significance toxicity in ICR mice[24]. The EtSCT was diluted in distilled water and administered via oral gavage for 5 days. After 5 days, the non-treated group was administered a constant volume of olive oil via intraperitoneal (i.p.) injection as a control, while the other three groups were given a single i.p. with a single dose of CCl_4 (0.6 ml/kg body weight diluted 1:10 in olive oil). At 24 hours after CCl_4 injection, the mice in each group were euthanized using a chamber filled with CO_2 gas, after which blood and organs were collected for further analysis.

Measurement of body and organ weight

The body weight of ICR mice was measured using an electronic balance (Mettler Toledo, Greifensee, Switzerland) every day during the experimental period according to the KFDA guidelines. In addition, the weights of six organs (liver, kidney, spleen, thymus, heart, and lung) collected from the sacrificed ICR mice were determined using the same method employed to measure the body weight.

Serum biochemistry

After the final injection of CCl_4, all ICR mice in each group were fasted for 8 hr, after which blood was collected from the abdominal veins and incubated for 30 min at room temperature. Whole blood was then centrifuged at 1,500 × g for 15 min to obtain the serum, after which biochemical components including alkaline phosphatase (ALP), alanine aminotransferase (ALT), aspartate aminotransferase (AST), and lactate dehydrogenase (LDH) were assayed using an automatic serum analyzer (Hitachi 747, Hitachi, Tokyo, Japan). All assays employed fresh serum and were conducted in duplicate.

Histological analysis

Liver tissue was dissected from mice and fixed in 4% neutral buffered formaldehyde (pH 6.8) overnight, after which each liver was dehydrated and embedded in paraffin. Next, a series of liver sections (4 μm) was cut from paraffin-embedded tissue using a Leica microtome (Leica Microsystems, Bannockburn, IL, USA). These sections were then deparaffinized with xylene, rehydrated with ethanol at a graded decreasing concentration of 100–70%, and finally washed with distilled water. The slides of liver sections were stained with hematoxylin & eosin (Sigma-Aldrich Corporation) and then washed with dH_2O, after which the necrotic area was measured in 1 mm^2 of each liver section using the Leica Application Suite (Leica Microsystems, Wetzlar, Germany).

Immunohistochemical analysis

Immunohistochemical analysis for the detection of collagen distribution using light microscopy was performed as previously described[25]. Briefly, liver tissue samples were fixed in 5% formalin for 12 h, embedded in paraffin and then sliced into 4 μm thick sections. These sections were subsequently deparaffinized with xylene, rehydrated, and pretreated for 30 min at room temperature with PBS blocking buffer containing 10% goat serum. Next, the sections were incubated with primary anti-collagen antibody (Abcam, Cambridge, MA, USA) diluted 1:1,000 in PBS blocking buffer. The antigen-antibody complexes were subsequently visualized with biotinylated secondary antibody (goat anti-rabbit)-conjugated HRP streptavidin (Histostain-Plus Kit, Zymed, South San Francisco, CA, USA) at a dilution of 1:1,500 in PBS blocking buffer. Finally, collagen proteins were detected using a stable DAB (Invitrogen Corp., Carlsbad, CA, USA) and the Leica Application Suite (Leica Microsystems, Switzerland).

Determination of MDA levels

The MDA levels were assayed using a Lipid Peroxidation (MDA) Assay Kit (Sigma-Aldrich Corporation) according to the manufacturer's protocols. The liver tissue was homogenized in MDA lysis buffer containing butylhydroxytoluene (BHT), after which the homogenates were stored at −20°C until analysis. The sample or standards and TBA solution (70 mM thiobarbituric acid and 5 M glacial acetic acid) were incubated at 95°C for 60 min and then cooled to room temperature in an ice bath for 10 min, after which the reaction absorbance at 532 nm was read using a VersaMax plate reader (Molecular Devices, Sunnyvale, CA, USA).

Western blot

Total proteins prepared from the liver tissue of mice were separated by 4–20% sodium dodecyl sulfate-polyacrylamide gel electrophoresis (SDS-PAGE) for 2 h, after which the resolved proteins were transferred to nitrocellulose membranes for 2 h at 40 V. Each membrane was then

incubated separately at 4°C overnight with the following primary antibodies: anti-Bcl2 (Abcam, Cambridge, UK), anti-Bax (Abcam), anti-caspase-3 (Cell Signaling Technology, Danvers, MA, USA), anti-MMP-1/8 (Santa Cruz Biotechnology, Inc., Dallas, TX, USA), anti-MMP-2 (Santa Cruz Biotechnology, Inc.), anti-MMP-9 (Santa Cruz Biotechnology, Inc.), anti-Smad 2/3 (Cell Signaling Technology), anti-p-Smad2/3 (Cell Signaling Technology), anti-p38 (Cell Signaling Technology), anti-p-p38 (Cell Signaling Technology), anti-SAPK/JNK (Cell Signaling Technology), anti-p-SAPK/JNK (Cell Signaling Technology), anti-SOD1 (Abcam), and anti-β-actin antibody (Sigma-Aldrich Corporation). The membranes were subsequently washed with washing buffer (137 mM NaCl, 2.7 mM KCl, 10 mM Na_2HPO_4, and 0.05% Tween 20) and incubated with horseradish peroxidase (HRP)-conjugated goat anti-rabbit IgG (Invitrogen Corp.) at a dilution of 1:1,000 for 1 h at room temperature. Membrane blots were developed using Amersham ECL Select Western Blotting detection reagent (GE Healthcare, Little Chalfont, UK).

Enzyme-linked immunosorbent assay (ELISA) for TGF-β1

The concentration of TGF-β1 in blood serum and liver tissue was measured using a TGF-β1 ELISA kit (BioLegend, San Diego, CA, USA) according to the manufacturer's protocols. After collection of serum and liver homogenate, the sample for analysis was prepared by adding acidification solution and neutralization solution to serum and liver tissue homogenate progressively. The mixtures of samples or standards between Assay Buffer C were incubated in a 96-well plate at room temperature for 2 h, while shaking at 200 rpm, after which 100 µl of TGF-β1 detection antibody solution was added to each well, and samples were then incubated at room temperature for 1 h with shaking. After washing, 100 µl of avidin-HRP-D solution was added to each well, and the plate was incubated at room temperature for 30 min with shaking. Next, 100 µl of substrate solution was added to each well, and the plate was incubated for 10 min in the dark. The reaction was then quenched by the addition of 100 µl of stop solution, after which the plates were analyzed by evaluation of the absorbance at 450 nm using a VersaMax plate reader (Molecular Devices).

RT-PCR

RT-PCR was conducted to measure the relative quantities of mRNA for anti- or pro-inflammatory cytokines including IL-1β, TNF-α, IL-6, and IL-10. Briefly, the liver tissues were chopped with scissors and homogenized in RNAzol solution (Leedo Medical Laboratories, Houston, TX, USA). The concentration of total isolated RNA was then measured by UV spectroscopy (BioSpec-Nano, Shimadzu Scientific Instruments, Columbia, MD, USA). Expression of inflammatory cytokines was assessed by RT-PCR with 3 µg of total RNA from the liver tissue of each group. Next, 500 ng of the oligo-dT primer (Invitrogen Corp.) was annealed at 70°C for 10 min. Complementary DNA, which was used as the template for further amplification, was synthesized by the addition of dATP, dCTP, dGTP, and dTTP with 200 units of reverse transcriptase. Next, 10 pM each of the sense and antisense primers were added, and the reaction mixture was subjected to 25–30 cycles of amplification in a PerkinElmer Thermal Cycler as follows: 30 sec at 94°C, 30 sec at 62°C, and 45 sec at 72°C. RT-PCR was also conducted using β-actin-specific primers to ensure RNA integrity. The primer sequences were as follows: 5′-GCA CAT CAA CAA GAG CTT CAG GCA G-3′, sense, and 5′-GCT GCT TGT GAG GTG CTG ATG TAC-3′, antisense, for IL-1β expression; 5′-CCT GTA GCC CAC GTC GTA GC-3′, sense, and 5′-TTG ACC TCA GCG CTG ACT TG-3′, antisense, for TNF-α expression; 5′-TTG GGA CTG ATG TTG TTG ACA-3′, sense, and 5′-TCA TCG CTG TTG ATA CAA TCA GA-3′, antisense, for IL-6 expression; 5′-CCA AGC CTT ATC GGA AAT GA-3′, sense, and 5′-TTT TCA CAG GGG AGA AAT CG-3′, antisense, for IL-10 expression; and 5′-GTG GGG CGC CCC AGG CAC CAG GGC-3′, sense, and 5′-CTC CTT AAT GTC ACG CAC GAT TT-3′, antisense, for β-actin expression. The experiment was repeated three times, and all samples were analyzed in triplicate. The final PCR products were separated by 1% agarose gel electrophoresis and visualized by ethidium bromide staining.

Statistical analysis

One-way ANOVA was used to identify significant differences between the non-treated and CCl_4-treated groups (SPSS Statistics for Windows, Version 10.10, Standard Version, SPSS Inc., Chicago, IL, USA). Additionally, differences between the Vehicle+CCl_4-treated group and the EtSCT+CCl_4-treated groups were evaluated by a *post hoc* test (SPSS Statistics for Windows, Version 10.10, Standard Version) of the variance and significance levels. All values were expressed as means ± SD. A P value of <0.05 was considered significant.

Results

Antioxidative properties of EtSCT

As shown in Table 1, total phenolic contents and flavonoids at 765 nm and 510 nm were 37.5 mg/g and 15.6 mg/g in EtSCT respectively. Moreover, DPPH radical scavenging activity was 93.3%, and NO scavenging activity was 15%, while metal chelation activity was 46.5%. The reducing power and SOD-like activity of EtSCT were 2.9% and 27%, respectively. These results demonstrate that EtSCT has good antioxidative properties that were likely related to its hepatoprotective effects.

No effects of EtSCT administration on body and organ weight

The effects of EtSCT administration on body and organ weight in ICR mice treated with CCl_4 were also evaluated. No significant difference in body weight was observed among groups throughout the 6 day experimental period, although their level was slightly lower in the LEtSCT+CCl_4-

Table 1. Components and Anti-oxidative Properties of EtSCT

Items	Concentration (mg/g)
Flavonoids	15.6 ± 1.03
Total phenolic contents	37.5 ± 2.07
Items	**Level (%)**
DPPH radical scavenging activity	93.3 ± 7.23
Metal chelation activity	46.5 ± 3.15
Reducing power	2.9 ± 0.18
NO scavenging activity	15.0 ± 0.96
SOD-like activity	27.0 ± 2.05

*DPPH, 2,2-diphenyl-1-picrylhydrazyl; NO, nitric oxide; SOD, superoxide dismutase.

Table 2. Alteration of Organ Weights of ICR Mice

Organs	Non-treated	CCl_4		
		Vehicle	LEtSCT	HEtSCT
Liver (g)	1.51 ± 0.107	1.39 ± 0.050	1.64 ± 0.669	1.40 ± 0.103
Kidney (g)	0.18 ± 0.014	0.19 ± 0.034	0.17 ± 0.012	0.18 ± 0.037
Spleen (g)	0.14 ± 0.016	0.10 ± 0.012[a]	0.11 ± 0.017[a]	0.11 ± 0.012[a]
Thymus (g)	0.13 ± 0.016	0.09 ± 0.026[a]	0.06 ± 0.018[a]	0.08 ± 0.013[a]
Heart (g)	0.18 ± 0.031	0.13 ± 0.016[a]	0.13 ± 0.030[a]	0.13 ± 0.017[a]
Lung (g)	0.26 ± 0.010	0.22 ± 0.023[a]	0.21 ± 0.027[a]	0.24 ± 0.033[a]

*The data are reported as the means ± SD of three replicates. [a]$P<0.05$ compared with the non-treated group.

Table 3. Alteration of Serum Parameters of ICR Mice

Parameters	Non-treated	CCl_4		
		Vehicle	LEtSCT	HEtSCT
ALT (U/L)	27.71 ± 2.13	31705.33 ± 7216.91[a]	22892.00 ± 5385.48[a,b]	19702.00 ± 4580.27[a,b]
AST (U/L)	79.57 ± 6.26	31211.00 ± 4493.98[a]	27236.00 ± 7455.75[a]	24268.00 ± 5013.45[a]
ALP (U/L)	124.00 ± 26.12	160.33 ± 32.55	173.33 ± 26.34[a]	212.57 ± 42.03[a,c]
LDH (U/L)	722.67 ± 196.35	17470.18 ± 6632.50[a]	10621.46 ± 420.86[a,b]	4751.81 ± 4262.69[b,c]

* The data are reported as the means ± SD of three replicates. [a]$P<0.05$ compared with the non-treated group. [b]$P<0.05$ compared with the vehicle+CCl_4-treated group. [c]$P<0.05$ compared with the LEtSCT+CCl_4-treated group.

treated group (Fig. 1B). Also, the liver and kidney weights did not show any significant differences between the non-treated group and EtSCT+CCl_4-treated groups (Table 2). However, the weights of the heart, lung, spleen, and thymus decreased after CCl_4 injection, and were not recovered in the LEtSCT+CCl_4- and HEtSCT+CCl_4-treated group when compared with the Vehicle+CCl_4-treated group (Table 2). These results indicate that EtSCT treatment for 5 days does not induce any significant change in body weight or the weight of most organs in ICR mice, which is different from ICR mice treated with only LEtSCT or HEtSCT[24].

Hepatoprotective effects of EtSCT on serum biochemical indicators

To examine the protective effects of EtSCT against CCl_4-induced toxicity in terms of serum biochemical indicators, the levels of liver indicators including ALP, AST, ALT, and LDH were measured in Vehicle+CCl_4- and EtSCT+CCl_4-treated ICR mice. The levels of AST, ALT, and LDH were higher in Vehicle+CCl_4-treated mice than in non-treated mice. Only two indicators (ALT and LDH) decreased significantly in a dose-dependent manner in EtSCT+CCl_4-treated mice compared with Vehicle+CCl_4-treated mice, although the rate of decrease varied for each factor. A slight decrease in AST was observed in the HEtSCT+CCl_4-treated group; however, this change was not significant. Additionally, the level of ALP was maintained at a constant level in the LEtSCT+CCl_4-treated group, and it was highly increased in the HEtSCT+CCl_4-treated group (Table 3). Taken together, these results show that pretreatment with EtSCT may suppress the increase in ALT and LDH induced by CCl_4 injection, although the ratio of decrease may vary according to each factor.

Protective effects of EtSCT on alteration of histopathology

Next, the protective effects of EtSCT during hepatocellular damage were identified by histological analysis of liver sections stained with hematoxylin and eosin. The histopathology of the liver in the non-treated group revealed a

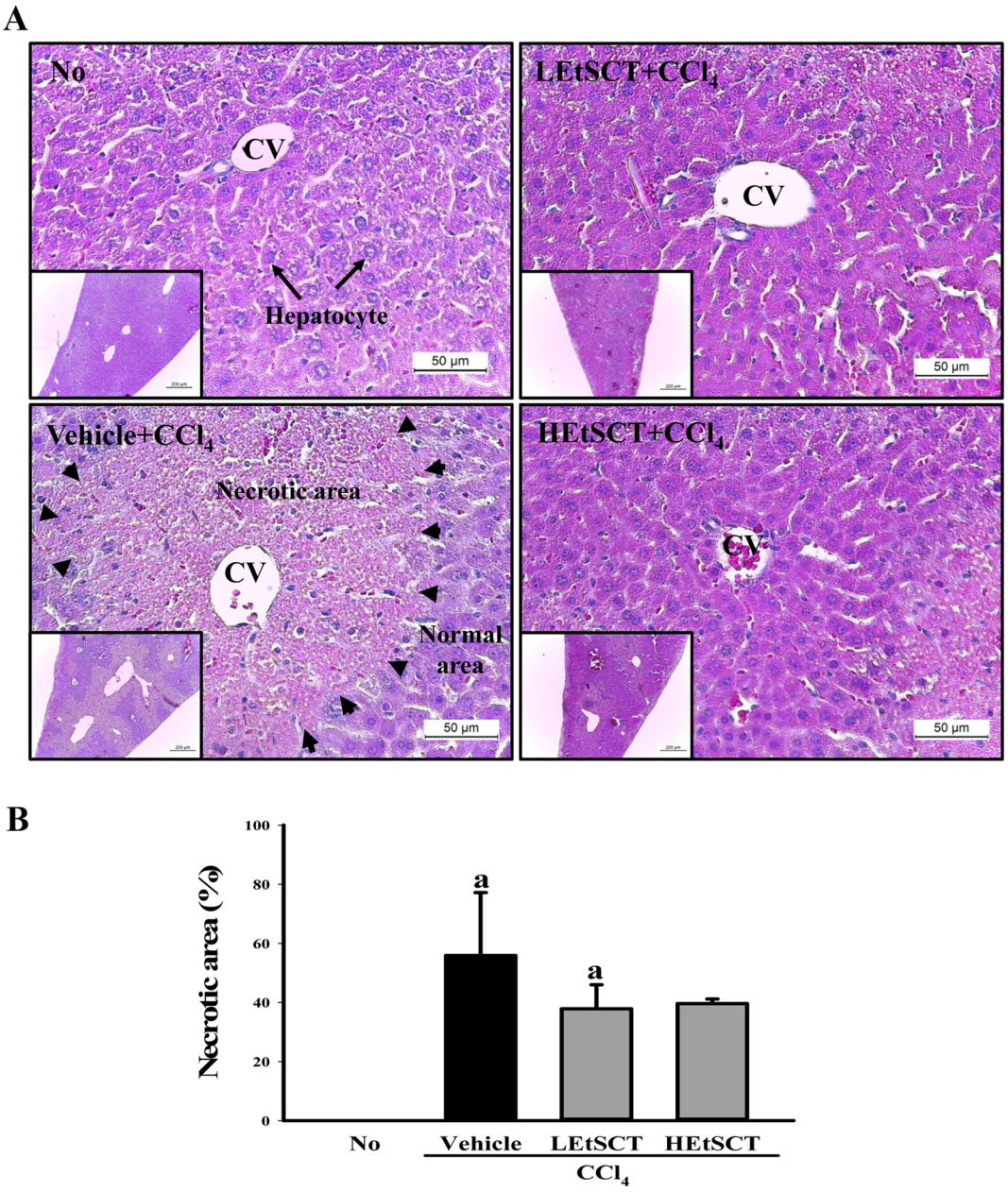

Fig. 2. Alteration of histopathology. (A) Severe centrilobular liver damage in the liver tissue section stained with H&E solution was clearly apparent around the central vein (CV) in the Vehicle+CCl_4-treated group, while the non-treated group showed no pathology. This damage was significantly recovered in the LEtSCT+CCl_4- and HEtSCT+CCl_4-treated groups. Histological alteration was observed around the enteral vein (CV) at a 400× magnification and at 100× magnification (left corner), which is shown in the corner of each image. (B) The necrotic area was measured in 1 mm^2 of each liver section using the Leica Application Suite (Leica Microsystems, Switzerland).

normal location for hepatocytes with clear visible nuclei, a portal triad, and a central vein. After CCl_4 treatment, extensive centrilobular necrosis was observed in and around the central vein (CV) of the liver. Furthermore, the CV in the liver section was dilated in the Vehicle+CCl_4-treated group relative to the non-treated group. However, the hepatocytes around the CV were reduced in the liver sections of EtSCT+CCl_4-treated groups, while the diameters of dilated CVs were partially recovered, becoming similar to those of non-treated group (Fig. 2A). The necrotic area around the CV of the liver decreased significantly, by 37.8–39.5% in the two EtSCT+CCl_4-treated groups (Fig. 2B). Taken together, these results indicate that EtSCT pretreatment may effectively inhibit changes in histopathology of the liver tissue induced by CCl_4 treatment.

Anti-apoptotic effects of EtSCT treatment

To examine if EtSCT pretreatment can prevent activation of apoptosis induced by CCl_4 exposure, the expression of apoptosis-related proteins was measured in total

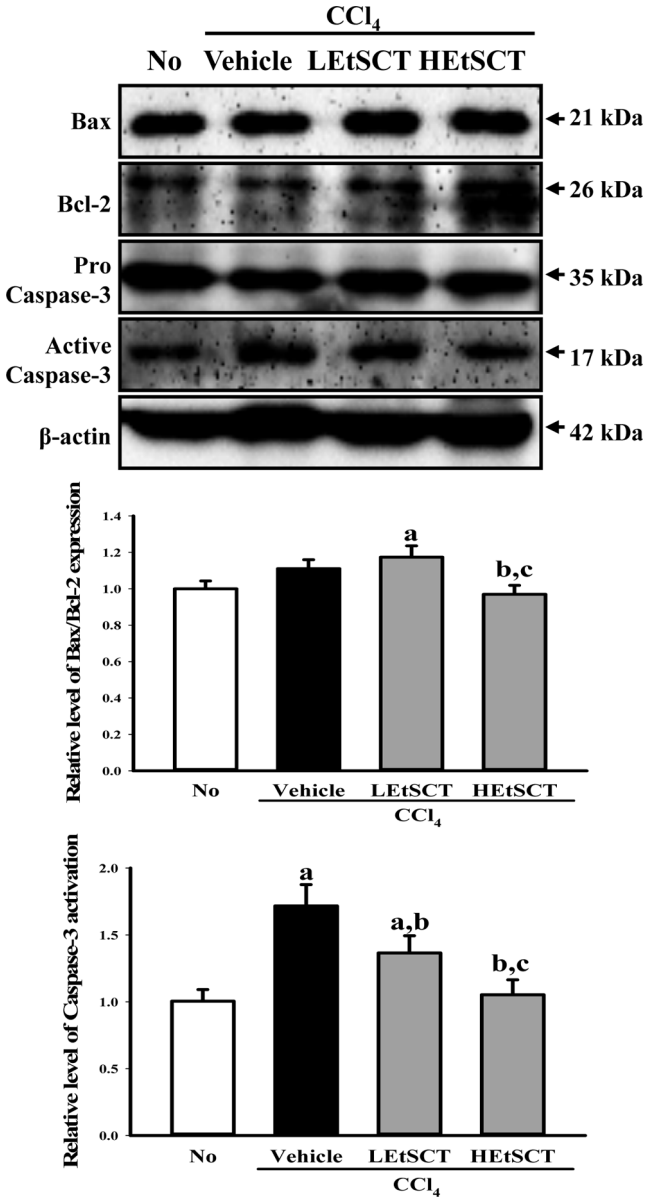

Fig. 3. Alteration of apoptosis-related proteins in the EtSCT+CCl_4-treated liver. Expression levels of caspase-3, Bcl-2, and Bax proteins in the liver tissue were analyzed using specific antibodies. Expression levels were quantified by an imaging densitometer and the sizes of the products indicated. Data represent the means ± SD of three replicates. [a]P<0.05 compared with the non-treated group. [b]P<0.05 compared with the Vehicle+CCl_4-treated group. [c]P<0.05 compared with the LEtSCT+CCl_4-treated group.

extract of the liver tissues of mice pretreated with EtSCT for 5 days. Among pro- and anti-apoptotic members of the BCl-2 family, the level of Bax/Bcl-2 expression was slightly higher in the Vehicle+CCl_4-treated group than the non-treated group. However, the level decreased significantly in the HEtSCT+CCl_4-treated groups relative to the Vehicle+CCl_4-treated group, while it increased slightly in the LEtSCT+CCl_4-treated group (Fig. 3). A similar pattern to that of the Bax/Bcl-2 expression was observed in the activation of caspase-3. Following CCl_4 injection, the pro-caspase-3 level was reduced, whereas the level of active caspase-3 increased by 171.6%. However, the levels of active caspase-3 decreased significantly, by 31.2–35.0% in the EtSCT+CCl_4-treated groups relative to the Vehicle+CCl_4-treated group (Fig. 3). Taken together, these results suggest that EtSCT pretreatment may protect against hepatocyte apoptosis induced by CCl_4 injection via regulation of Bax/Bcl-2 expression and caspase-3 activation.

Anti-inflammation effects of EtSCT treatment

We next investigated whether EtSCT pretreatment could induce alterations in the transcription levels of anti- and pro-inflammatory cytokines. To accomplish this, the transcription levels of IL-10, IL-1β, IL-6, and TNF-α were measured in the subset groups by RT-PCR analysis. The expression of the four cytokines was very similar in the subset group. The levels of these cytokines were 10.1–240.3% higher in the Vehicle+CCl_4-treated group than in the non-treated group. However, the levels decreased in a dose-dependent manner in the EtSCT+CCl_4-treated groups, although the rate of decrease varied. The highest decrease of IL-1β (300%) and lowest decrease (9.88%) of IL-10 were detected in the HEtSCT+CCl_4-treated group (Fig. 4A). These results indicated that EtSCT pretreatment can inhibit the increase of anti- and pro-inflammatory cytokines induced by CCl_4 injection.

To determine if downregulation of TNF-α mRNA was accompanied by alterations in the downstream signaling pathway, the phosphorylation levels of the key proteins in the pathway were measured in the liver tissue. Interestingly, the phosphorylation level of p38 significantly increased in the two EtSCT+CCl_4-treated groups even though the Vehicle+CCl_4-treated group showed very low levels (Fig. 4B). However, the phosphorylation level of JNK was maintained at a constant level, regardless of the concentration of EtSCT. Taken together, these results suggest that the TNF-α signaling pathway activated by EtSCT pretreatment was closely related to the regulation of p38 phosphorylation.

Protective effects of EtSCT against hepatic fibrosis

Hepatic fibrosis, which is a histological hallmark of chronic liver disease, is characterized by excessive accumulation of connective tissue in the liver and considered an indicator of persistent or progressive hepatic injury[26]. In a previous study, dense staining of an excessive accumulation of collagen that expanded into the portal triads was observed in a Vehicle+CCl_4-treated group compared with a non-treated group[27]. To investigate the protective effects of EtSCT against CCl_4-induced hepatic fibrosis, samples were evaluated for changes in collagen and MMPs expression, and TGF-β1 signaling pathways were observed in the liver tissue of the subset groups. The collagen protein was densely stained around the portal triad of the Vehicle+CCl_4-treated group relative to the non-treated group in the immunohistochemical analysis. However, this accumula-

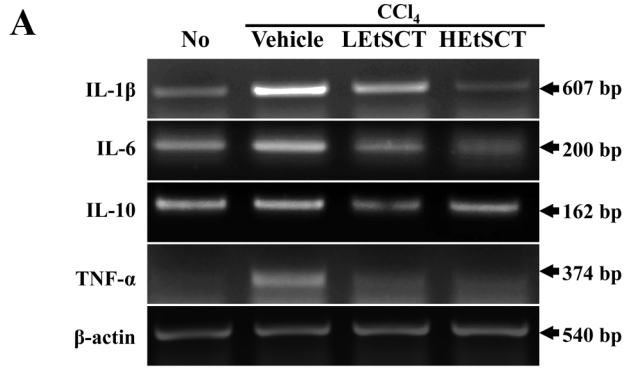

Expression level of cytokine	Control	Vehicle	LEtSCT	HEtSCT
IL-1β	1.0±0.05	3.4±0.37[a]	1.7±0.15[a,b]	0.4±0.01[a,b,c]
IL-6	1.0±0.07	1.1±0.11[a]	0.7±0.05[a,b]	0.6±0.02[a,b]
IL-10	1.0±0.06	0.9±0.06	0.5±0.04[a,b]	0.8±0.18[a,b,c]
TNF-α	1.0±0.01	1.6±0.09[a]	1.0±0.04[b]	0.9±0.01[b]

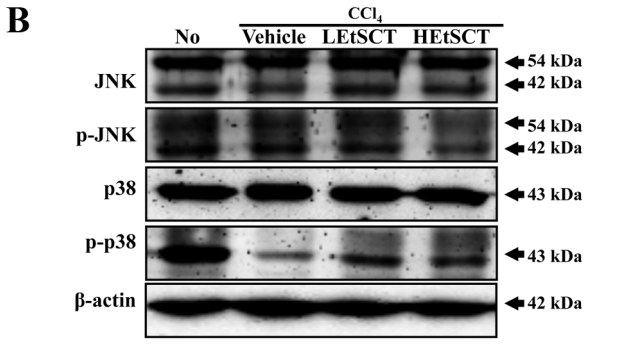

Phophorylation level of protein	Control	Vehicle	LEtSCT	HEtSCT
JNK	1.0±0.03	0.9±0.04	0.9±0.03	0.9±0.01
p38	1.0±0.06	0.2±0.01[a]	0.4±0.02[a,b]	0.5±0.28[a,b,c]

Fig. 4. Alteration of inflammatory cytokines and the TNF-α downstream signaling pathway in the EtSCT+CCl_4-treated liver. (A) mRNA level of pro-inflammatory and anti-inflammatory cytokines in the non-treated, Vehicle+CCl_4-treated, and EtSCT+CCl_4-treated groups. After purification of total RNA from the liver tissues of mice in each group, the mRNA levels of the TNF-α, IL-1β, IL-6, and IL-10 genes were examined by RT-PCR using specific primers. (B) Phosphorylation levels of p38 and JNK in liver tissue. The phosphorylation levels of the two proteins were calculated to divide the phosphorylated protein levels into the unphosphorylated protein levels. Three mice per group were assayed by western blotting. Values are reported as means ± SD. [a]$P<0.05$ compared with the non-treated group. [b]$P<0.05$ compared with the Vehicle+CCl_4-treated group. [c]$P<0.05$ compared with the LEtSCT+CCl_4-treated group.

tion significantly decreased in the HEtSCT+CCl_4-treated group (Fig. 5A). Furthermore, the expression of MMP-1 was higher in the Vehicle+CCl_4-treated group than in the non-treated group, but it was significantly decreased in the HEtSCT+CCl_4-treated group relative to the Vehicle+CCl_4-treated group, while the opposite was observed for the expression of MMP-2 and MMP-9. The decreases in these proteins after Vehicle+CCl_4 treatment were recovered in the LEtSCT+CCl_4- and HEtSCT+CCl_4-treated group (Fig. 5D). Additionally, the concentrations of TGF-β1 in the serum and liver tissue were 20–172.4% higher in the Vehicle+CCl_4-treated group than in the non-treated group. These levels were recovered to those of the non-treated group in the two EtSCT+CCl_4-treated groups, even though great recovery was detected in the liver tissue homogenate. Furthermore, a recovery pattern similar to that of the TGF-β1 concentration was observed in the serum (Fig. 5B). The Samd2/3 phosphorylation level in the TGF-β1 signaling pathway fully reflected the alteration of the TFG-β1 concentration in the subset groups. However, these levels were significantly decreased in a dose-dependent manner in the LEtSCT+CCl_4- and HEtSCT+CCl_4-treated group (Fig. 5C). Overall, the above results suggest that EtSCT pretreatment can induce a decrease in TGF-β1 secretion through regulation of Smad2/3 activation.

Protective effects of EtSCT on the regulation of oxidative stress

Finally, to examine the protective effects of EtSCT on the oxidative stress induced by CCl_4 exposure, the MDA concentration and SOD expression were measured in the liver tissue. A significant increase in the MDA concentration (282.8%) was detected in the Vehicle+CCl_4-treated group relative to the non-treated group. After EtSCT treatment, the levels of the two EtSCT-treated groups were significantly decreased (by 71.0% and 81.7%; Fig. 6A).

Conversely, a pattern opposite to that of the MDA concentrations was observed upon analysis of SOD expression. The Vehicle+CCl_4-treated group showed a significantly lower level of SOD expression than that of the non-treated group. However, the level was recovered to that of the non-treated group by EtSCT pretreatment (Fig. 6B). Taken together, these results indicate that EtSCT pretreatment may inhibit the oxidative stress induced by CCl_4 exposure through suppression of lipid peroxidation and increased SOD repression.

Discussion

In liver pathology, free radicals induce oxidative stress that can lead to fatty degeneration, inflammation, fibrosis, hepatocellular death, and carcinogenicity[28, 29]. Therefore, effective removal of free radicals has been considered one strategy for treatment of liver injury. To achieve this, some natural products from various marine organisms are being investigated as important sources for the prevention of diseases associated with oxidative stress, even though various drugs have already been used in the treatment of hepatic disorders[30–38]. Recently, several compounds and extracts of the SCT have received a great deal of attention as novel therapeutic mixture candidates because of their antioxidant properties. A number of related studies are currently being conducted to identify their novel functions and mechanisms

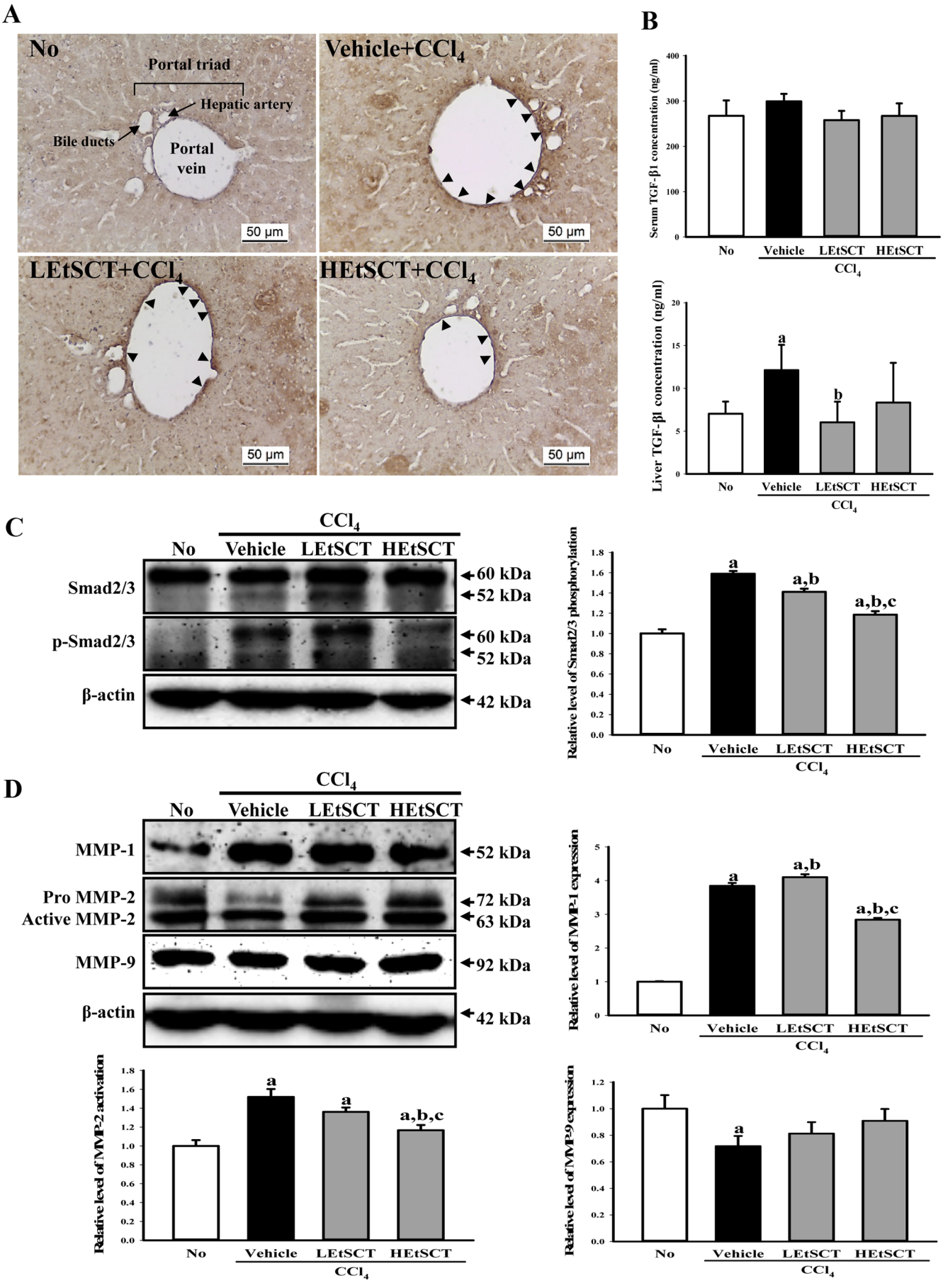
A
No
Portal triad
Hepatic artery
Bile ducts
Portal vein
50 μm
Vehicle+CCl4
LEtSCT+CCl4
HEtSCT+CCl4
B
Serum TGF-β1 concentration (ng/ml)
Liver TGF-β1 concentration (ng/ml)
No
Vehicle
LEtSCT
HEtSCT
CCl4
C
Smad2/3
p-Smad2/3
β-actin
60 kDa
52 kDa
42 kDa
Relative level of Smad2/3 phosphorylation
D
MMP-1
Pro MMP-2
Active MMP-2
MMP-9
72 kDa
63 kDa
92 kDa
Relative level of MMP-1 expression
Relative level of MMP-2 activation
Relative level of MMP-9 expression

Fig. 5.

of action[39, 40]. In an effort to develop drugs for the treatment of oxidative stress-induced diseases, we investigated the protective effects of EtSCT against hepatic injury in ICR mice after CCl_4 exposure. Our results demonstrated that EtSCT pretreatment was associated with relief of liver inflammation and fibrosis through the suppression of oxidative stress induced by CCl_4 treatment.

Several reactive intermediates such as trichloromethyl radical ($CCl_3^{\bullet}$) and trichloromethyl peroxy radical ($CCl_3OO^{\bullet}$) were produced by activation of cytochrome P450 in liver tissue after CCl_4 injection[29]. These radicals can bind to cellular molecules (nucleic acids, proteins, and lipids), impairing lipid metabolism, inducing membrane dysfunction, and initiating hepatic cancer[41]. To prevent the hepatic damages induced by CCl_4 treatment, it is important to identify compounds and extracts with high antioxidant activity that originate from natural products. Therefore, the EtSCT used in this study can likely relate with to its hepatoprotective effects because it has good ability for antioxidative properties.

The results of serum marker enzyme analysis following treatment with EtSCT were consistent with those of several previous studies that showed that administration of similar SCT extracts resulted in significant recovery of pathological symptoms, including serum marker enzymes, in CCl_4-treated animals. Water-ethanol extracts of the Ascidian purple sea squirt (*Halocynthia aurantium*) increased the threshold of erythrocyte hemolysis resistance and stimulated the preservation of lipid composition in the erythrocyte membrane[42]. Moreover, the administration of an ethanol extract of an Ascidian (*Microcosmus exasperatus*) restored the increases in SGPT, SGOT, ALP, and total bilirubin levels and the activities of GPX, DOS, and GSH in CCl_4-treated Wistar rats[43]. However, these studies did not show their effects on hepatic inflammation, apoptosis, or fibrosis. The results of the present study provide the first evidence of the molecular action mechanism of EtSCT leading to hepatoprotective effects in CCl_4-induced liver damage.

Meanwhile, liver toxicity was confirmed based on alterations in the levels of four enzymes (ALP, ALT, AST, and LDH) related to liver metabolism[44]. Among them, the ALP level in serum can be increased by large bile duct obstruction, intrahepatic cholestasis, or infiltrative diseases of the liver[45]. When liver toxicants such as CCl_4 are administered to animals, the damaged liver cells release a large amount of ALP into the blood[46]. In this study, the serum level of ALP was gradually enhanced in the Vehicle+CCl_4-, LEtSCT+CCl_4- and HEtSCT+CCl_4-treated group compared with the non-treated group, although Vehicle+CCl_4 did not show any statistical significance. However, the results of our previous study showed that EtSCT did not induce any toxic effects on liver tissue of EtSCT-treated mice without CCl_4 based on the serum levels of four enzyme indicators and histological structure[24]. Therefore, we believe that an increase in only the ALP level in the LEtSCT+CCl_4- and HEtSCT+CCl_4-treated groups may have been correlated with the synergistic effects of some EtSCT components and CCl_4 on the hepatic injury, as hemolysis of red blood cells during collection of whole blood was previously shown to simultaneously enhance the ALP and AST levels[47]. However, the present study provides limited information, as total extracts of SCT and CCl_4 were administered to ICR mice. Furthermore, more studies are necessary to clarify the synergistic effect of combinational complex between individual component and CCl_4.

Two different apoptosis pathways lead to caspase activation, the mitochondrial pathway and the death-receptor pathway[48]. Among them, the mitochondrial pathway is regulated by the Bcl-2 family of proteins, which consist of anti-apoptotic (such as Bcl-2) and pro-apoptotic (such as Bax) proteins[32]. Although CCl_4 injection induced caspase-3 activation and cytochrome c release within the mitochondrial pathway in apoptotic hepatocytes[49, 50], this apoptotic damage has been protected against by administration of various antioxidant mixtures including *Salvia miltiorrhiza*, dibenzoyl glycoside from *Salvinia natans*, dioscin, glycyrrhizic acid, and the flavonoid fraction from *Rosa laevigata Michx* fruit[51–54]. The above effects on the regulation of apoptotic proteins detected in previous studies were also observed in the present study. As shown in Fig. 3, the ratio of Bax/Bcl-2 expression and caspase-3 activation increased significantly in the Vehicle+CCl_4-treated group, but they were restored in the EtSCT+CCl_4-treated groups. Therefore, these findings indicate that EtSCT can be considered important candidates to prevent and treat the damage induced by apoptotic inducers such as oxidative stress and toxic chemicals.

The toxic metabolites produced by CCl_4 injection can stimulate the secretion of cytokines including IL-1, TNF-α, and TGF-β through regulation of redox-sensitive transcription factors such as NFκB, activator protein 1 (AP-1), and early growth response 1 (EGR1) in Kupffer cells[29, 55, 56]. In

Fig. 5. Alteration of regulatory factors of liver fibrosis in EtSCT+CCl_4-treated mice. (A) Immunohistochemistry of collagen protein. After CCl_4 treatment, the collagen proteins were detected as a dense line around portal vein of portal triads compared with the non-treated group, but the levels were decreased in the same region in HEtSCT+CCl_4-treated mice. Histological alteration was observed around the portal triads stained with specific antibody at 400× magnification. (B) ELISA for TGF-β1. After preparation of blood serum and liver tissue homogenate, the concentration of TGF-β1 was determined in the two different mixtures using a TGF-β1 ELISA kit that could detect TGF-β1 at 3.5 pg/mL. (C) Western blot analysis for Smad2/3 expression. To measure the expression levels of Smad2/3 and p-Smad2/3 protein, membranes were incubated with specific antibodies for each protein, as well as β-actin protein from liver lysates. Three mice per group were assayed by western blotting. (D) Western blot analysis of MMP-1, 2, and 9 expression. To measure the expression levels of MMP proteins, the membranes were incubated with specific antibodies for each protein, as well as β-actin protein from liver lysates. Three mice per group were assayed by western blotting. Values are reported as the means ± SD. [a]$P<0.05$ compared with the non-treated group. [b]$P<0.05$ compared with the Vehicle+CCl_4-treated group. [c]$P<0.05$ compared with the LEtSCT+CCl_4-treated group.

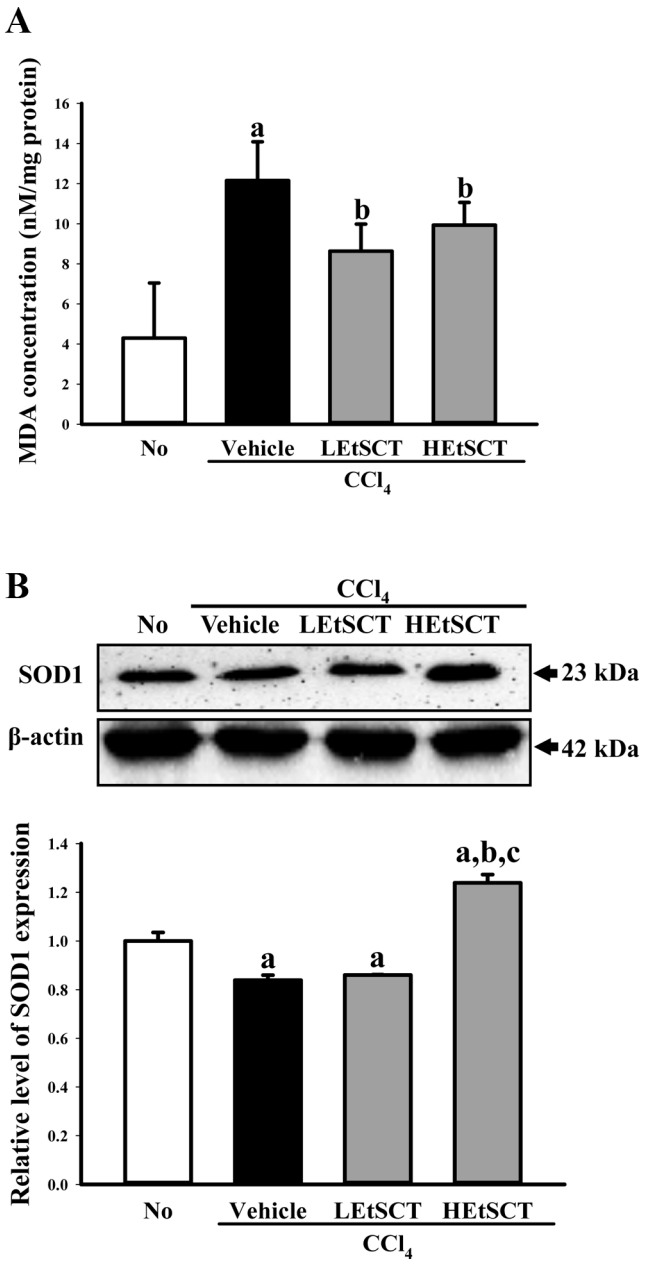

Fig. 6. Analysis of oxidant stress-related factors in EtSCT+CCl_4-treated mice. (A) The level of MDA was determined in serum collected from mice using a lipid peroxidation assay kit that could detect MDA at 0.1 nmol/mg to 20 nmol/mg. (B) The expression level of SOD was measured in the homogenates of liver tissue collected from subset groups. The intensity of each band was determined using an imaging densitometer, and the relative level of each protein was calculated based on the intensity of actin protein as an endogenous control. Data represent the means ± SD of three replicates. [a]$P<0.05$ compared with the non-treated group. [b]$P<0.05$ compared with the Vehicle+CCl_4-treated group. [c]$P<0.05$ compared with the LEtSCT+CCl_4-treated group.

CCl_4-treated animals, the TNFα and IL-6 concentrations increased significantly, but these levels were inhibited by several compounds and mixtures, including curcumin, polysaccharide from *Tarphochlamys affinis* (PTA), and ursolic acid[57–59]. Furthermore, the expression of an anti-inflammatory cytokine (IL-10) was increased in the serum of Balb/c mice with CCl_4-induced liver injury[60] or decreased in the hepatic supernatant of SD rats with CCl_4-induced liver injury[2]. The IL-10 level was also significantly reduced by pretreatment with ruxolitinib (15 mg/kg) for 2 h[60], but it did not change in response to treatment with ginseng extract and ginsenoside Rb1 for 2 weeks in CCl_4-treated animals[2]. In the present study, the expression of pro- and anti-inflammatory cytokines was dramatically decreased by EtSCT pretreatment in a dose-dependent manner, which was similar to the results of previous studies, although a few differences in expression levels of cytokines were detected. These differences were likely a result of variations in the properties of bioactive compounds and the genetic background of the experimental animals used among studies.

A variety of damages, such as that resulting from chronic exposure of CCl_4, viral hepatitis infections such as hepatitis B virus (HBV) and hepatitis C virus (HCV) infections, or administration of metabolic agents, induce liver fibrosis, which is characterized by excessive accumulation of extracellular matrix (ECM) through abnormal regulation of connective tissue synthesis and ECM homeostasis[61, 62]. Several mixtures and bioactive compounds, including Fufang-Liu-Yue-Qing, epigallocatechin-3-gallate (EGCG), silymarin, and curcumin[58, 63–65] effectively improved the severity of hepatic fibrosis in mice and rats treated with toxicants including CCl_4, although there were no attempts to apply SCT-related products. Furthermore, the synthesis and secretion of collagen leading to increased scar formation in ECM can be activated by the Smad-dependent pathway after stimulation with TGF-β1[66]. The TGF-β1 concentration and collagen expression were significantly reduced in response to treatment with most of the above herbs or compounds[30, 58, 63, 64]. In the present study, the EtSCT-treated groups showed restoration of collagen expression, the TGF-β1 concentration, and MMP-1 expression. Most of our results regarding liver fibrosis were similar to those of previous studies. However, the increase in MMP-2/9 in the EtSCT-treated groups differed from that in previous studies. Accordingly, additional studies should be conducted to determine what other factors regulate MMP-2/9 expression.

The free radicals derived from CCl_4 in hepatic injury can react with membrane lipids, leading to their peroxidation[41]. Many antioxidant compounds and mixtures such as MCL, polysaccharide from Angelica and Astragalus (AAP), ellagitannin-enriched *Melaleuca styphelioides* Sm. (Myrtaceae), and *Fagonia schweinfurthii* (Hadidi) Hadidi (Family: Zygophyllaceae) significantly reduced the increase of lipid peroxides induced by CCl_4 injection[67–70]. Extracts from the Ascidian tunic within subphylum Urochordata affected the lipid content in the whole blood of animals. Serum cholesterol, neutral lipids, phospholipids, and LDL-cholesterol were decreased in SD rats treated with Ascidian insoluble cellulose[71], while conservation of the lipid components ratio in the erythrocyte membrane was promoted by treatment

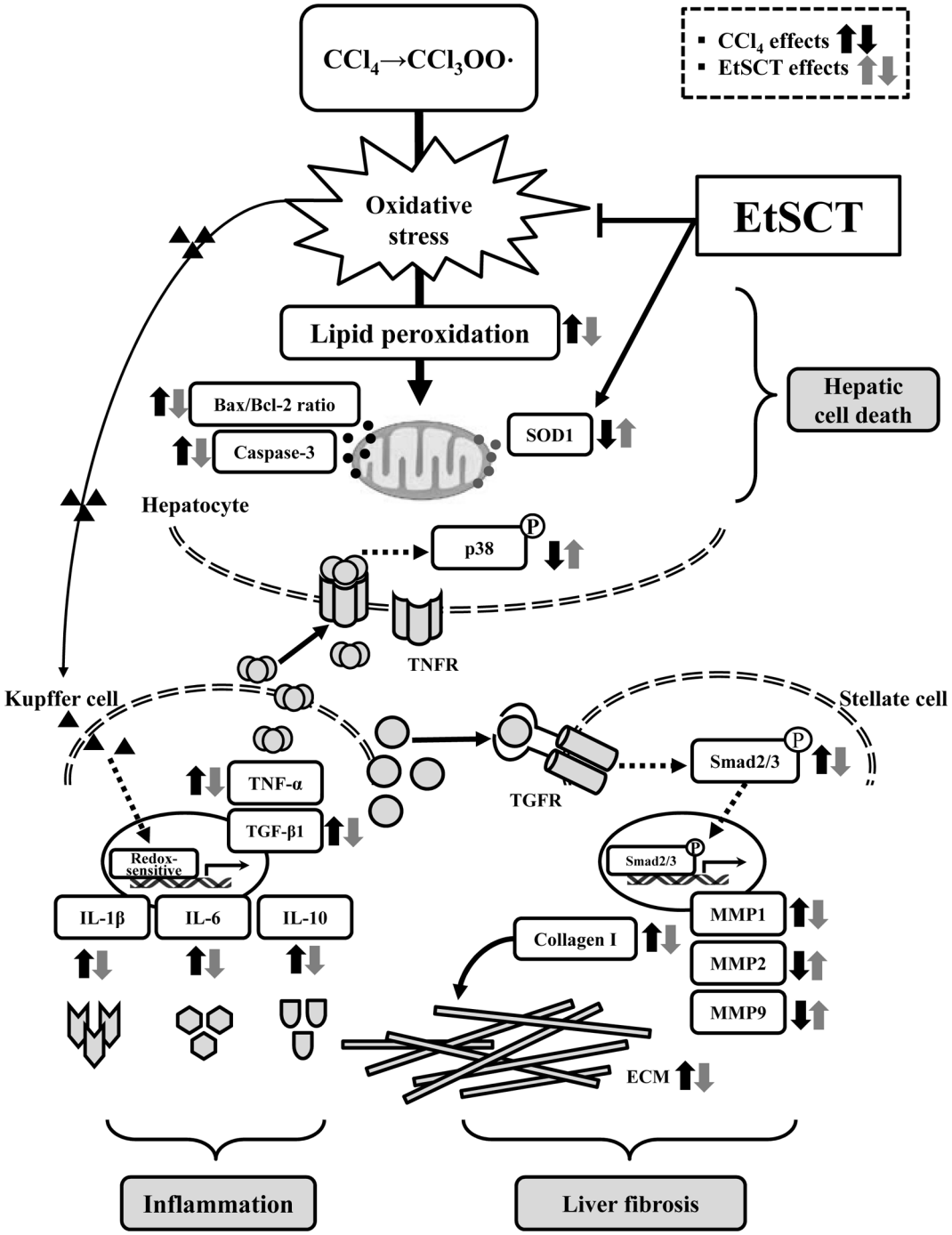

Fig. 7. Suggested mechanism of EtSCT action in CCl_4-induced hepatic injury. In this scheme, the protective effects of EtSCT are thought to be exerted via the suppression of hepatic apoptosis, inflammation, and liver fibrosis induced by CCl_4 injection through the inhibition of lipid peroxidation and apoptosis in hepatocytes, the TNF-α signaling pathway in Kupffer cells, and the TGF-β signaling pathway in stellate cells.

with a water-ethanol extract of the Ascidian purple sea squirt[40]. In this study, pretreatment with EtSCT significantly improved antioxidative conditions, including lipid peroxidation and SOD expression (Fig. 6). These findings provided evidence that the hepatoprotective effects of EtSCT may be tightly associated with the effects of antioxidant activity on lipid peroxidation and SOD expression.

Taken together, the results of the present study indicate that EtSCT effectively protects against CCl_4-induced hepatic injury in ICR mice. EtSCT pretreatment prevented the increase of serum marker enzymes, enhancing hepatic apoptosis and necrosis, liver fibrosis, and inflammation through the suppression of lipid peroxidation and induction of antioxidant enzyme expression (Fig. 7). Therefore, our

study provides a solution for the environmental problem of increasing SCT wastes via their use as novel bioactive materials.

Acknowledgments: We thank Jin Hyang Hwang, the animal technician, for directing the care of experimental animal at the Laboratory Animal Resources Center. This study was supported by grants to Dr. Dae Youn Hwang from the Korea Institute of Planning Evaluation for Technology of Food, Agriculture, Forestry and Fisheries (112088-03 and 116027032HD030). This study was financially supported by the "2017 Post-Doc. Development Program" of Pusan National University.

Disclosure of Potential Conflicts of Interest: The authors declare that they have no conflicts of interest.

References

1. Bataller R, and Brenner DA. Liver fibrosis. J Clin Invest. **115**: 209–218. 2005. [Medline] [CrossRef]
2. Hou YL, Tsai YH, Lin YH, and Chao JC. Ginseng extract and ginsenoside Rb1 attenuate carbon tetrachloride-induced liver fibrosis in rats. BMC Complement Altern Med. **14**: 415–425. 2014. [Medline] [CrossRef]
3. Rockey D, and Friedman S. Hepatic fibrosis and cirrhosis. In: Zakim and Boyer's hepatology, Vol. 1 5th ed. Boyer TD, Wright TL, Manns MP (eds). Elsevier, New York. 87–109. 2006.
4. Fattovich G, Stroffolini T, Zagni I, and Donato F. Hepatocellular carcinoma in cirrhosis: incidence and risk factors. Gastroenterology. **127**(Suppl 1): S35–S50. 2004. [Medline] [CrossRef]
5. Hernandez-Gea V, and Friedman SL. Pathogenesis of liver fibrosis. Annu Rev Pathol. **6**: 425–456. 2011. [Medline] [CrossRef]
6. Berasain C, Castillo J, Perugorria MJ, Latasa MU, Prieto J, and Avila MA. Inflammation and liver cancer: new molecular links. Ann N Y Acad Sci. **1155**: 206–221. 2009. [Medline] [CrossRef]
7. Cragg GM, and Newman DJ. Drug discovery and development from natural products: the way forward. 11th NAPRECA Symposium Book of Proceedings. 56–69. 2005.
8. Ahn SH, Jung SH, Kang SJ, Jeong TS, and Choi BD. Extraction of glycosaminoglycans from *Styela clava* tunic. Biotechnol Bioproc Eng. **18**: 180–185. 2003.
9. Lee SM, Kang EJ, Go TH, Jeong SY, Park GT, Lee HS, Hwang DY, Jung YJ, and Son HJ. Screening of biological activity of solvent extract from *Styela clava* tunic for fishery waste recycling. J Environ Sci Inte. **23**: 89–96. 2014. [CrossRef]
10. Jung YJ. Properties of regenerated cellulose films prepared from the tunicate *Styela clava*. J Kor Fish Soc. **4**: 237–242. 2008.
11. Jung YJ, An BJ, Hwang DY, Kim HD, Park SM, Cho H, and Kim HS. Preparation and properties of regenerated cellulosic biomaterial made from *Styela clava* tunics. J Biomed Mater Res. **12**: 71–76. 2008.
12. Kwak MH, Go J, Kim JE, Lee YJ, Lee SH, Lee HS, Son HJ, Jung YJ, and Hwang DY. Property and efficacy analysis of hydrocolloid membrane containing *Styela clava* tunic on the wound repair of skin in SD rats. Biomat Res. **17**: 91–101. 2013.
13. Kim SM, Lee JH, Cho JA, Lee SC, and Lee SK. Development of a bioactive cellulose membrane from sea squirt skin for bone regeneration – A preliminary research. J Korean Assoc Oral Maxillofac Surg. **31**: 440–453. 2005.
14. Xu CX, Jin H, Chung YS, Shin JY, Woo MA, Lee KH, Palmos GN, Choi BD, and Cho MH. Chondroitin sulfate extracted from the *Styela clava* tunic suppresses TNF-α-induced expression of inflammatory factors, VCAM-1 and iNOS by blocking Akt/NF-kappaB signal in JB6 cells. Cancer Lett. **264**: 93–100. 2008. [Medline] [CrossRef]
15. Nacional LM, Kang SJ, and Choi BD. Antioxidative activity of carotenoids in Mideodeok *Styela clava*. Fisher Aquat Sci. **14**: 243–249. 2011. [CrossRef]
16. Song SH, Kim JE, Lee YJ, Kwak MH, Sung GY, Kwon SH, Son HJ, Lee HS, Jung YJ, and Hwang DY. Cellulose film regenerated from *Styela clava* tunics have biodegradability, toxicity and biocompatibility in the skin of SD rats. J Mater Sci Mater Med. **25**: 1519–1530. 2014. [Medline] [CrossRef]
17. Singleton VL, and Rossi JA. Colorimetry of total phenolics with phosphomolybdic-phosphotungstic acid reagents. Am J Enol Vitic. **16**: 144–158. 1965.
18. Zhishen J, Mengcheng T, and Jianming W. The determination of flavonoid contents in mulberry and their scavenging effects on superoxide radicals. Food Chem. **64**: 555–559. 1999. [CrossRef]
19. Oh H, Ko EK, Kim DH, Jang KK, Park SE, Lee HS, and Kim YC. Secoiridoid glucosides with free radical scavenging activity from the leaves of *Syringa dilatata*. Phytother Res. **17**: 417–419. 2003. [Medline] [CrossRef]
20. Oyaizu M. Studies on products of the browning reaction. Antioxidative activities of browning reaction products prepared from glucosamine. Jpn J Nutr. **44**: 307–315. 1986. [CrossRef]
21. Marcocci L, Maguire JJ, Droy-Lefaix MT, and Packer L. The nitric oxide-scavenging properties of *Ginkgo biloba* extract EGb 761. Biochem Biophys Res Commun. **201**: 748–755. 1994. [Medline] [CrossRef]
22. Dinis TCP, Maderia VM, and Almeida LM. Action of phenolic derivatives (acetaminophen, salicylate, and 5-aminosalicylate) as inhibitors of membrane lipid peroxidation and as peroxyl radical scavengers. Arch Biochem Biophys. **315**: 161–169. 1994. [Medline] [CrossRef]
23. Marklund S, and Marklund G. Involvement of the superoxide anion radical in the autoxidation of pyrogallol and a convenient assay for superoxide dismutase. Eur J Biochem. **47**: 469–474. 1974. [Medline] [CrossRef]
24. Koh EK, Sung JE, Kim JE, Go J, Song SH, Lee HA, Son HJ, Jung YJ, Lim Y, and Hwang DY. Toxicity of antioxidative extract collected from *Styela clava* tunics in ICR mice. Lab Anim Res. **31**: 125–133. 2015. [Medline] [CrossRef]
25. Hwang DY, Chae KR, Kang TS, Hwang JH, Lim CH, Kang HK, Goo JS, Lee MR, Lim HJ, Min SH, Cho JY, Hong JT, Song CW, Paik SG, Cho JS, and Kim YK. Alterations in behavior, amyloid beta-42, caspase-3, and Cox-2 in mutant PS2 transgenic mouse model of Alzheimer's disease. FASEB J. **16**: 805–813. 2002. [Medline] [CrossRef]
26. Bissell DM. Cell-matrix interaction and hepatic fibrosis. Prog Liver Dis. **9**: 143–155. 1990. [Medline]
27. Go J, Kim JE, Koh EK, Song SH, Sung JE, Lee HA, Lee

YH, Lim Y, Hong JT, and Hwang DY. Protective effect of gallotannin-enriched extract isolated from Galla Rhois against CCl_4-induced hepatotoxicity in ICR mice. Nutrients. **8**: 107–127. 2016. [Medline] [CrossRef]
28. Luster MI, Simeonova PP, Gallucci RM, Bruccoleri A, Blazka ME, and Yucesoy B. Role of inflammation in chemical-induced hepatotoxicity. Toxicol Lett. **120**: 317–321. 2001. [Medline] [CrossRef]
29. Weber LW, Boll M, and Stampfl A. Hepatotoxicity and mechanism of action of haloalkanes: carbon tetrachloride as a toxicological model. Crit Rev Toxicol. **33**: 105–136. 2003. [Medline] [CrossRef]
30. Li L, Li W, Kim YH, and Lee YW. *Chlorella vulgaris* extract ameliorates carbon tetrachloride-induced acute hepatic injury in mice. Exp Toxicol Pathol. **65**: 73–80. 2013. [Medline] [CrossRef]
31. Hsu YW, Tsai CF, Chang WH, Ho YC, Chen WK, and Lu FJ. Protective effects of *Dunaliella salina*, a carotenoids-rich alga, against carbon tetrachloride-induced hepatotoxicity in mice. Food Chem Toxicol. **46**: 3311–3317. 2008. [Medline] [CrossRef]
32. Lee TY, Chang HH, Wang GJ, Chiu JH, Yang YY, and Lin HC. Water-soluble extract of *Salvia miltiorrhiza* ameliorates carbon tetrachloride-mediated hepatic apoptosis in rats. J Pharm Pharmacol. **58**: 659–665. 2006. [Medline] [CrossRef]
33. Yeh YH, Hsieh YL, Lee YT, and Hu CC. Protective effects of *Geloina eros* extract against carbon tetrachloride-induced hepatotoxicity in rats. Food Res Int. **48**: 551–558. 2012. [CrossRef]
34. Hwang HJ, Kim IH, and Nam TJ. Effect of a glycoprotein from *Hizikia fusiformis* on acetaminophen-induced liver injury. Food Chem Toxicol. **46**: 3475–3481. 2008. [Medline] [CrossRef]
35. Bupesh IG, Amutha C, Vasanth S, Manoharan N, Senthil Raja R, Krishnamoorthy R, and Subramanian P. Hepatoprotective efficacy of *Hypnea muciformis* ethanolic extract on CCl_4 induced toxicity in rats. Braz Arch Biol Technol. **55**: 857–863. 2012. [CrossRef]
36. Esmat AY, Said MM, Soliman AA, El-Masry KS, and Badiea EA. Bioactive compounds, antioxidant potential, and hepatoprotective activity of sea cucumber (*Holothuria atra*) against thioacetamide intoxication in rats. Nutrition. **29**: 258–267. 2013. [Medline] [CrossRef]
37. Karthikeyan R, Somasundaram ST, Manivasagam T, Balasubramanian T, and Anantharaman P. Hepatoprotective activity of brown alga *Padina boergesenii* against CCl_4 induced oxidative damage in wistar rats. Asian Pac J Trop Med. **3**: 696–701. 2010. [CrossRef]
38. Raghavendran HB, Sathivel A, Yogeeta RSSK, and Devaki T. Efficacy of *Sargassum polycystum* (Phaeophyceae) sulphated polysaccharide against paracetamol-induced DNA fragmentation and modulation of membrane-bound phosphatases during toxic hepatitis. Clin Exp Pharmacol Physiol. **34**: 142–147. 2007. [Medline] [CrossRef]
39. Park JH, Seo BY, Lee SC, and Park EJ. Effects of ethanol extracts from stalked sea squirt (*Styela clava*) on antioxidant potential, oxidative DNA damage and DNA repair. Food Sci Biotechnol. **19**: 1035–1040. 2010. [CrossRef]
40. Seo BY, Jung ES, Kim JY, Park HR, Lee SC, and Park EJ. Effect of aceton extract from *Styela clava* on oxidative DNA damage and anticancer activity. J Korean Soc Appl Biol Chem. **49**: 227–232. 2006.
41. Singh N, Kamath V, Narasimhamurthy K, and Rajini PS. Protective effect of potato peel extract against carbon tetrachloride-induced liver injury in rats. Environ Toxicol Pharmacol. **26**: 241–246. 2008. [Medline] [CrossRef]
42. Fomenko SE, Kushnerova NF, and Lesnikova LN. Experimental assessment of the efficiency of erythrocyte membrane repair by an extract of the tunic of the ascidian purple sea squirt in carbon tetrachloride poisoning. Pharm Chem J. **46**: 606–611. 2013. [CrossRef]
43. Meenakshi VK, Gomathy S, Senthamarai S, Paripooranaselvi M, and Chamundeswari KP. Hepatoprotective activity of the ethanol extract of simple ascidian, *Microcosmus exasperatus* Heller, 1878. Eur Jour Zoo Res. **2**: 32–38. 2013.
44. Shimizu Y. Liver in systemic disease. World J Gastroenterol. **14**: 4111–4119. 2008. [Medline] [CrossRef]
45. Siddique A, and Kowdley KV. Approach to a patient with elevated serum alkaline phosphatase. Clin Liver Dis. **16**: 199–229. 2012. [Medline] [CrossRef]
46. Kim DH, Deung YK, Lee YM, Yoon YS, Kwon KR, Park DB, Park YK, and Lee KJ. The liver protecting effect of Pomegranate (*Punica granatum*) seed oil in mice treated with CCl_4. Korean J Electron Microscopy. **36**: 173–182. 2006.
47. Koseoglu M, Hur A, Atay A, and Cuhadar S. Effects of hemolysis interferences on routine biochemistry parameters. Biochem Med (Zagreb). **21**: 79–85. 2011. [Medline] [CrossRef]
48. Araragi S, Kondoh M, Kawase M, Saito S, Higashimoto M, and Sato M. Mercuric chloride induces apoptosis via a mitochondrial-dependent pathway in human leukemia cells. Toxicology. **184**: 1–9. 2003. [Medline] [CrossRef]
49. Sun F, Hamagawa E, Tsutsui C, Ono Y, Ogiri Y, and Kojo S. Evaluation of oxidative stress during apoptosis and necrosis caused by carbon tetrachloride in rat liver. Biochim Biophys Acta. **1535**: 186–191. 2001. [Medline] [CrossRef]
50. Brown GC, and Borutaite V. Nitric oxide, cytochrome c and mitochondria. Biochem Soc Symp. **66**: 17–25. 1999. [Medline] [CrossRef]
51. Srilaxmi P, Sareddy GR, Kavi Kishor PB, Setty OH, and Babu PP. Protective efficacy of natansnin, a dibenzoyl glycoside from *Salvinia natans* against CCl_4 induced oxidative stress and cellular degeneration in rat liver. BMC Pharmacol. **10**: 13–25. 2010. [Medline] [CrossRef]
52. Lu B, Xu Y, Xu L, Cong X, Yin L, Li H, and Peng J. Mechanism investigation of dioscin against CCl_4-induced acute liver damage in mice. Environ Toxicol Pharmacol. **34**: 127–135. 2012. [Medline] [CrossRef]
53. Guo XL, Liang B, Wang XW, Fan FG, Jin J, Lan R, Yang JH, Wang XC, Jin L, and Cao Q. Glycyrrhizic acid attenuates CCl_4-induced hepatocyte apoptosis in rats via a p53-mediated pathway. World J Gastroenterol. **19**: 3781–3791. 2013. [Medline] [CrossRef]
54. Zhang S, Lu B, Han X, Xu L, Qi Y, Yin L, Xu Y, Zhao Y, Liu K, and Peng J. Protection of the flavonoid fraction from *Rosa laevigata* Michx fruit against carbon tetrachloride-induced acute liver injury in mice. Food Chem Toxicol. **55**: 60–69. 2013. [Medline] [CrossRef]
55. Ramadori G, and Armbrust T. Cytokines in the liver. Eur J Gastroenterol Hepatol. **13**: 777–784. 2001. [Medline] [CrossRef]
56. Simeonova PP, Gallucci RM, Hulderman T, Wilson R,

Kommineni C, Rao M, and Luster MI. The role of tumor necrosis factor-α in liver toxicity, inflammation, and fibrosis induced by carbon tetrachloride. Toxicol Appl Pharmacol. **177**: 112–120. 2001. [Medline] [CrossRef]
57. Reyes-Gordillo K, Segovia J, Shibayama M, Vergara P, Moreno MG, and Muriel P. Curcumin protects against acute liver damage in the rat by inhibiting NF-kappaB, proinflammatory cytokines production and oxidative stress. Biochim Biophys Acta. **1770**: 989–996. 2007. [Medline] [CrossRef]
58. Lin X, Liu X, Huang Q, Zhang S, Zheng L, Wei L, He M, Jiao Y, Huang J, Fu S, Chen Z, Li Y, Zhuo L, and Huang R. Hepatoprotective effects of the polysaccharide isolated from *Tarphochlamys affinis* (Acanthaceae) against CCl_4-induced hepatic injury. Biol Pharm Bull. **35**: 1574–1580. 2012. [Medline] [CrossRef]
59. Ma JQ, Ding J, Zhang L, and Liu CM. Ursolic acid protects mouse liver against CCl_4-induced oxidative stress and inflammation by the MAPK/NF-κB pathway. Environ Toxicol Pharmacol. **37**: 975–983. 2014. [Medline] [CrossRef]
60. Hazem SH, Shaker ME, Ashamallah SA, and Ibrahim TM. The novel Janus kinase inhibitor ruxolitinib confers protection against carbon tetrachloride-induced hepatotoxicity via multiple mechanisms. Chem Biol Interact. **220**: 116–127. 2014. [Medline] [CrossRef]
61. Friedman SL, Maher JJ, and Bissell DM. Mechanisms and therapy of hepatic fibrosis: report of the AASLD Single Topic Basic Research Conference. Hepatology. **32**: 1403–1408. 2000. [Medline] [CrossRef]
62. Wells RG. The role of matrix stiffness in hepatic stellate cell activation and liver fibrosis. J Clin Gastroenterol. **39**(Suppl 2): S158–S161. 2005. [Medline] [CrossRef]
63. Tipoe GL, Leung TM, Liong EC, Lau TY, Fung ML, and Nanji AA. Epigallocatechin-3-gallate (EGCG) reduces liver inflammation, oxidative stress and fibrosis in carbon tetrachloride (CCl_4)-induced liver injury in mice. Toxicology. **273**: 45–52. 2010. [Medline] [CrossRef]
64. Mata-Santos HA, Lino FG, Rocha CC, Paiva CN, Castelo Branco MT, and Pyrrho AS. Silymarin treatment reduces granuloma and hepatic fibrosis in experimental schistosomiasis. Parasitol Res. **107**: 1429–1434. 2010. [Medline] [CrossRef]
65. Fu Y, Zheng S, Lin J, Ryerse J, and Chen A. Curcumin protects the rat liver from CCl_4-caused injury and fibrogenesis by attenuating oxidative stress and suppressing inflammation. Mol Pharmacol. **73**: 399–409. 2008. [Medline] [CrossRef]
66. Ihn H. Autocrine TGF-beta signaling in the pathogenesis of systemic sclerosis. J Dermatol Sci. **49**: 103–113. 2008. [Medline] [CrossRef]
67. Sahreen S, Khan MR, and Khan RA. Hepatoprotective effects of methanol extract of *Carissa opaca* leaves on CCl_4-induced damage in rat. BMC Complement Altern Med. **11**: 48–56. 2011. [Medline] [CrossRef]
68. Pu X, Fan W, Yu S, Li Y, Ma X, Liu L, Ren J, and Zhang W. Polysaccharides from *Angelica* and *Astragalus* exert hepatoprotective effects against carbon-tetrachloride-induced intoxication in mice. Can J Physiol Pharmacol. **93**: 39–43. 2015. [Medline] [CrossRef]
69. Al-Sayed E, El-Lakkany NM, Seif El-Din SH, Sabra AN, and Hammam OA. Hepatoprotective and antioxidant activity of *Melaleuca styphelioides* on carbon tetrachloride-induced hepatotoxicity in mice. Pharm Biol. **52**: 1581–1590. 2014. [Medline] [CrossRef]
70. Pareek A, Godavarthi A, Issarani R, and Nagori BP. Antioxidant and hepatoprotective activity of *Fagonia schweinfurthii* (Hadidi) Hadidi extract in carbon tetrachloride induced hepatotoxicity in HepG2 cell line and rats. J Ethnopharmacol. **150**: 973–981. 2013. [Medline] [CrossRef]
71. Yook HS, Kim JO, Choi JM, Kim DH, Cho SK, and Byun MW. Changes of nutritional characteristics and serum cholesterol in rats by the intake of dietary fiber isolated from ascidian (*Hlocynthia roretzi*) tunic. Korean J Nutr. **32**: 474–478. 2003.